Environmental Science: Nano RSCPublishing

ARTICLE

†Electronic Supplementary Information (ESI) available: [Influence of different types of natural organic matter on titania nanoparticles stability: effects of counter ion concentration and pH]

Table S1. Review of other work related to aggregation of TiO2 NP.

Reference	Particles type, initial size and concentration	NOM	Electrolytes, pH and temp	Type of measurement for stability and interaction with NOM - instrument	Results and analysis
Chen, et al. [1]	TiO_2 nominal diameter 10x40nm. 20 mg/L	SRHA 0-10 mg/L	NaCl 3-200 mM pH 5.7 and 9 buffered with 0.4 mM $NaHCO_3$ and 0.1 mM Na_2CO_3	UV-vis spectrophotometry for measuring residual SRHA after contact with TiO_2. Zeta potential measurements.	More SRHA is lost from the solution (adsorbed or degraded) at larger NaCl concentration. At pH 9 SRHA was as effective stabilizing the particles as it was at pH 5.7 Zeta potential of TiO_2 more negative with more SRHA added.
Chowdhury, et al. [2]	TiO_2 6, 13 and 23 nm nominal dry diameters. DLS diameters in 1mM KCl at pH 7: 411, 512, 442 nm; at pH 10: 182, 146, 181 nm.	SRHA 1-10 mg/L	KCl, IS 1-100 mM $CaCl_2$, IS 1-100 mM pH 7 and 10	EPM; 1 mg/L attachment efficiencies – tr-DLS (KCl); SLS for aggregate morphology.	IEP previously reported as 3.5. All EPM were negative except at pH 7 with 100mM $CaCl_2$ for TiO_2 NP 6 and 13 nm. CCC in KCl (no pH indicated; perhaps 7): 30, 60 and 100 mM for 6, 13 and 23 nm repectivley. Df at pH 7 were higher than at pH 10. Linear relationship between aggregate morphology and surface areas of primary nanoparticles. Df are intensity averaged for all particles present, therefore high polydispersity and many low size particles may lead to overestimation of the fractal dimensions.
Domingos, et al. [3]	TiO_2 nominal size 5 nm, 1 mg/L, equlibrated 24 h. Bare particles labeled with Rodhamine 6G; FCS diameter w/o SRFA 8, 24, 29 nm and w/ SRFA 13, 26, 15 nm at pH 4, 6 and 8.	SRFA 1 mg/L. No Rodhamine	$CaCl_2$ 0.1 – 3.3 mM Na_2HPO_4, 0.001 – 0.1 mM	FCS and EPM at different values of pH, ionic composition and concentrations of SRFA (only for PO_4^{-3})	w/o SRFA more negative EPM with PO_4^{-3} addition. No difference w/ SRFA. No clear trend with $CaCl_2$. IEP of bare particles at pH 4.5-5.2. Increased particle size with addition of electrolytes but always remaining < 100nm. Aggregation tendency pH 8>6>4. PO_4^{-3} induced less aggregation than $CaCl_2$ in bare particles.
Domingos, et al. [4]	TiO_2 nominal size 5 nm. 1 g/L labeled with Rodhamine 110 (theoretically 1% coverage) or	SRFA 0.2-5 mg/L	IS 5-100 mM pH 2-8	Aggregation behaviour, 1mg/L. FCS measurements and electrophoretic mobility	1 mgL^{-1} SRFA caused charge inversion even at pH 2

Reference	Particles type, initial size and concentration	NOM	Electrolytes, pH and temp	Type of measurement for stability and interaction with NOM - instrument	Results and analysis
	SRFA			at different concentrations of SRFA, pH and IS.	
French, et al. [5]	Synthesized TiO_2 NP. TEM primary particle size 5 nm. Adjusted to pH 4.3-4.8 and filtered (0.45 um): intensity-peak hydrodynamic diameter ~50-60 nm		NaCl 45 mM, 85 mM, 125 mM, and $CaCl_2$ 16.5 mM at pH 4.3 and 4.8, respectively. At other pH values the starting aggregate size was much higher.	Aggregation rates; ~40 mg/L TiO_2. DLS intensity weighed size distributions are presented.	High aggregation even at the early times
Keller, et al. [6]	TiO_2 primary size 27 nm; DLS size in water 194 nm CeO2 rods primary size 67x8 nm; DLS size in water 231 nm ZnO primary size 24 nm; DLS size in water 205 nm 10, 50, 100, 200 mg/L	10 water samples TOC (uM C): three seawaters (50-130); lagoon (522); groundwater (842); River water (164); WWTP effluent (378); mesocosm freshwater (5283) and wastewater (691.8): stormwater runoff (1564)	10 water samples with IS from 3 meq/L (mesocosm wastewater) – 700 meq/L (seawater)	DLS measurements. Time resolved UV-vis spectrophotometry (concentration). EPM measurements at 10 mg/L in 1mM KCl.	IEP: TiO_2 pH 6.2; CeO_2 pH 7.5; ZnO pH 9.2 Seawater destabilized the particles much more than any other water. This allowed calculating apparent attachment coefficients dividing by the sedimentation rate of seawater. High TOC and low IS stabilized the NP. TiO_2<CeO_2<ZnO. Unknown if it is related to number concentration or concomitant dissolution.
Labille, et al. [7]	TiO_2 core 10x50nm; $Al(OH)_3$ layer and outer coating of PDMS. 400 mg/L aged during 48h at dark and light conditions. The colloidal by-product suspensions (48 h settling; 25% remained in colloidal form and this was diluted 4 times) were analysed for stability.	Dextran (neutral, MW 2E06 Da), Gellan (anionic, MW 3E06 Da), YAS34 (anionic, MW 2 MDa). Lower MW: humic and tannic acid.	NaCl 1-100 mM NaCl $MgCl_2$ 0.1-10 mg/L pH of the aged solution 6.3	IEP for the colloidal by-product suspension. Turbidity measurements for stability after addition of electrolytes to the diluted colloidal by-product suspension and settling 24 h.	The IEP of the colloidal by-product suspensions were 8 and 7.3 under dark and light conditions, respectively. CCC's were 20 mM NaCl and 8 mM $MgCl_2$ for both dark and light conditions. 2%wt NOM destabilized the particles but 20% stabilized them depending on NOM quality.
Li and Sun [8]	TiO_2 primary size 30 nm. DLS diameters larger than 1000 nm for all pH conditions tested. 50 mg/L were used in the experiments.	SRFA: monosystem (0-5 mg/L as TOC); binary system (0.5-2.5 mg/L as TOC)	Fe(III): mono- and binary system 0-0.2 mM. pH adjusted to 4, 5, 6 and 8 with 0.1 M HCl	24 h stirring at 200 RPM. EPM DLS z-average. UV-vis spectrophotometry (concentration) for measuring	Decrease in EPM at concentrations > 0.5 mg/L SRFA. Stable aggregates at ~400 nm at conc. > 1.5mg/L SRFA. Increase in EPM at conc. Fe(III) > 0.025mM. Possible charge inversion at 0.05

Reference	Particles type, initial size and concentration	NOM	Electrolytes, pH and temp	Type of measurement for stability and interaction with NOM - instrument	Results and analysis
			or NaOH	sedimentation rates. FTIR to prove complexation of Fe(III) to SRFA. XPS to determine chemical states and binding energies of each element in the samples.	and 0.15 mM for pH 6 and 8, respectively. In presence of SRFA there is an increase of EPM but instability remains because of proximity to zero. XPS confirmed the presence of Fe(III)-hydroxy complex in some cases. FTIR confirmed the complexation of Fe(III) to SRFA, probably reducing the effect of the Fe(III) ion on stability. Sedimentation experiments correlated with the stability ranges for EPM and size measurements.
Liu, et al. [9]	TiO_2 Nominal diameters 5, 10 and 50 nm anatase NP and 10x40 and 30x40 nm rutile NP. 20 mg/L with DLS size at pH 7 165, 369, 146, 181, 542 nm, respectively.		NaCl 1 – 1000 mM $CaCl_2$ 0.1 – 10 mM	Microwave assisted digestion and ICP-OES for determination of impurities. UV-vis spectrophotometry (concentration) for measuring sedimentation rates. 20 mg/L TiO_2; Attachment efficiencies – TR-DLS. EPM and IEP.	IEP based on EPM measurements were at pH 6, 6, 2.7, 4.4 and 4.7, respectively. According to sedimentation rates, stability at pH 7 is 10nm<5nm<10x40nm<50nm. CCC: non-stable, 5, 10 and 18 mM NaCl and non-stable, 0.3, 0.5 and 1 mM $CaCl_2$ for 10, 5, 10x40 and 50 nm NP.
Liu, et al. [10]	TiO_2 primary size 30 nm. Titanate NT, outer diameter 8 nm, inner diameter 5nm and hundreds of nm in length. Titanate– TiO_2 NT similar structure but shorter lengths with TiO_2 incrustations. 50 mg/L suspensions were used; no	SRHA 0-10 mg TOC/L (fixed pH 6 and IS 10 mM)	NaCl and $CaCl_2$; IS between 0 and 25 mM (fixed pH 6). pH adjusted with NaOH or HCl from 2 to 9 (fixed IS 10 mM). 25 C	EPM and IEP DLS z-average. UV-vis spectrophotometry (concentration) for measuring sedimentation rates.	IEP for TiO_2, NT and TiO_2-NT 6.5, 2.6 and 2.9. IS 10 mM from Ca^{2+} shifted all EPM towards positive values except for both NT at pH > 6. SRHA reduced the EPM to negative values even at low SRHA conc (1 mg TOC/L) and in presence of 10 mM IS from Ca^{2+}. Sedimentation experiments correlapted with the stability ranges for EPM and size measurements.
Liu, et al. [11]	TiO_2 nominal 21nm. CeO_2 nominal 15nm. Initial concentration 20 mg/L (stabilized in the respective pH)		pH 3-10 adjusted with NaOH, HCl and $NaHCO_3$ IS 0.01 – 1 mM with	DLS measurements and zeta potential (0.1 M IS) on stock suspensions at pH 3, 8 and 10.	Simulated particle diameter (unspecified) correlated well with the “stable” particle size in the range tested.

Reference	Particles type, initial size and concentration	NOM	Electrolytes, pH and temp	Type of measurement for stability and interaction with NOM - instrument	Results and analysis
	with average DLS size 170nm and 300nm for TiO_2 and CeO_2, respectively.		NaCl.		
Loosli, et al. [12]	TiO_2 anatase in suspension 170 g/L. Experiments performed at 50 mg/L with thorough stirring.	SRHA 100 mg/L Alginate 100 mg/L	IS 1 mM adjusted with NaCl. pH adjusted before and during the experiments: 2 to 11	EPM and DLS z-average diameter at 50 mg/L TiO_2. IEP EPM and DLS z-average diameter of 100 mg/L Alginate and SRHA.	Equilibration times varied between 45 min for Alginate and 24 h for SRHA (100 mg/L). z-average at pH 3 to 11 of SHRA and Alginate 379nm and 178nm, respectively. IEP of TiO_2 NP at pH 6.2 At pH<IEP: Stable TiO_2 NP at Alginate and SRHA concentrations > 1.7mg/L and > 2.8 mg/L respectively. At pH=IEP: Stable TiO_2 NP at Alginate and SRHA concentrations > 3mg/L and > 5 mg/L respectively. At pH>IEP: Stable TiO_2 NP at all concentrations; Alginate and TiO2 NP don't interact; sorption of SRHA is limited.
Mudunkotuwa and Grassian [13]	TiO_2 anatase nominal diameter 5 nm. No wet diameter reported in final solutions. Stock solutions were 2 g/L with intensity mode diameter at ~500 nm (pH 2).	Citric acid 0- 0.2mM	pH 2 – 10 mM HCl pH 4 – 0.1 mM HCl pH 6 – 25 mM MES pH 7.5 – 25 mM HEPES For aggregation studies ionic strength was adjusted to 30 mM with NaCl.	IEP with 50 mg/L TiO_2, 0 and 0.1 mM ctric acid and ionic strength 30 mM. Monitoring change in light scattering in UV-vis as a function of time (sedimentation) 2 g/L. Aggregate sizes of DLS (time frame not specified) as a function of citric acid concentration; 10 mg/L TiO_2 and 0-0.2 mM citric acid.	IEP 4.2 without and below 3 with citric acid. Aggregation was favoured in the presence of citric acid at pH 2 and stabilized the particles at pH 6, contrary to the behaviour in absence of citric acid. Adsorption of citric acid onto 4 nm (dry powder diameter) TiO_2 nanoparticles is pH dependant and irreversible. Saturation occurred at concentrations larger than 2 mM.
Ottofuelling, et al. [14]	TiO_2 P-25 nominal 21 nm. At 25 mg/L and pH different from IEP, DLS diameter 300 nm.	Seven natural waters filtered through 0.2um filter; DOC values (mg/L): groundwater (1.6), lake water (2.1), tap	Seven natural waters. Stability tests with NaCl, $CaCl_2$, Na_2SO_4 and $CaSO_4$.	DLS, turbidity (concentration) and zeta potential measurements after 18 hours.	NOM gave stability to the particles. Most natural waters presented unstable conditions. Notable exceptions were the ones with high DOC content. Some regions of positive zeta potential with

Reference	Particles type, initial size and concentration	NOM	Electrolytes, pH and temp	Type of measurement for stability and interaction with NOM - instrument	Results and analysis
		water (1.0), peat bog water (37.2), wastewater (67.5), outflow from WWTP (10.1), and seawater (<0.5). Three EPA synthetic water with DOC <0.5 mg/L. Stability tests probably with SRNOM			$CaCl_2$ and $CaSO_4$ at various pH suggest charge inversion.
Shih, et al. [15]	Synthesized TiO_2 NP. 31 nm starting zeta-average diameter; TEM diameter ~ 12 nm spheroids.		NaCl 0-1000 mM, Na_2SO_4 0-250 mM and $CaCl_2$ 0-200 mM; original pH conditions 3; 25 C	Initial aggregation kinetics; 1 g/L TiO_2; attachment efficiencies – TR-DLS; Zeta potential Vs pH and electrolyte concentration	TR-DLS CCC at pH 3: NaCl 340mM, $CaCl_2$ 145 mM and Na_2SO_4 0,7 mM Slight charge inversion with Na_2SO_4 < 1 mM at pH 3. IEP at pH 7.1
Shih, et al. [16]	Stabilized commercial TiO_2 NP; nominal size 7 nm. DLS z-average 66 nm		pH 3-4. NaCl 0-1000 meq/L and Na_2SO_4 0-100 meq/L.	1 g/L TiO2; Attachment efficiencies – TR-DLS; Zeta potential Vs pH and electrolyte concentration	DLS-CCC at pH 3: Cl^{-1} 300meq/L and SO_4^{-2} 2 meq/L IEP at pH 6.4
Sillanpää, et al. [17]	TiO_2 P-25 nominal diameter 21 nm. 1 g/L ~200 nm DLS diameter.	2 fresh water and 2 brackish water samples filtered through 0.45 um.	Brackish waters pH~8 Freshwaters pH 6.1 and 5	Aggregation rates, 1 and 100 mg/L. DLS zeta-average UV-vis spectrophotometer for TiO_2 NP concentrations in sedimentation experiments.	One freshwater favoured the stabilisation of TiO_2-P25 over the other: pH, Ca, Mg, SO4, TOC in mg/L 5, 0.7, 0.3, 2.7, 6.1 6.1, 1.7, 0.7, 5.4, 4.1 Lower aggregation rate at lower initial particle concentration.
Solovitch, et al. [18]	TiO_2 nominal diameter 32 nm. Dispersed at pH 2.5 at concentration 50 mg/L; DLS diameter 150 nm.		NaCl 1 – 1000 mM NaCl at pH 8 and 5 for TR-DLS. pH 3 – 9 for IEP.	EPM and IEP 50 mg/L; attachment efficiencies – TR-DLS.	CCC's were 1-10 mM and 10-40 mM NaCl for pH 5 and 8, respectively. IEP at around pH 5.2.
Thio, et al. [19]	TiO_2 primary size 27 nm; DLS size for 100 mg/L in water 194 nm	SRHA 0, 10 mg/L	NaCl 1, 10 and 100 mM $CaCl_2$ 0.01, 0.05, 0.1, 1, 10 mM Borate buffer 1 mM	10 mg/L; attachment efficiencies – TR-DLS.	At pH 8 CCC NaCl, NaCl+SRHA, $CaCl_2$, $CaCl_2$+SRHA => 15, 200, 0.1 and 5 mM respectively. Zeta potential increasing with salt concentration. For $CaCl_2$ at 1mM negative

Reference	Particles type, initial size and concentration	NOM	Electrolytes, pH and temp	Type of measurement for stability and interaction with NOM - instrument	Results and analysis
			pH 5, 6, 7, 8 and 9		at pH 7 and 8 and positive for pH 5, 6, and 9. For $CaCl_2$ 10 and 100 mM positive at all pH.
von der Kammer, et al. [20]	TiO_2 P-25 nominal 21 nm and TiO_2 UV-100 nominal <10 nm. Z-average 293 ± 16 and 302 ± 43 nm when dispersed 50 mg/L in water, respectively.	SRNOM	NaCl, Na_2SO_4, $CaCl_2$ and Sodium diphosphate as positive control. Unbuffered pH.	Aggregation rates; 1 sampling point measuring NP concentration (as turbidity) and zeta potential as a function of pH and concentration of electrolyte or polyelectrolyte (NOM). 50 mg/L TiO_2 with starting size > 200 nm depending on pH	Several regions of stability found with Na_2SO_4 and $CaCl_2$ suggesting charge inversion by divalent counterions. NOM and diphosphate stabilize the particles at almost all pH levels including pH=PZC.
Yang, et al. [21]	SiO_2 (20 and 30 nm), TiO_2 50 nm, Al_2O_3 (150 and 60 nm) and ZnO (20 nm). 5 g/L stock dispersions prepared in the HA solutions. No hydrodynamic diameter reported.	Peat soil HA 50-1500 mg/L for NP coating 10-200 mg/L for Adsorption	pH 5	2 days equilibration of 5 g/L NP with HA solutions. EPM and IEP of diluted dispersions to 50 mg/L. FTIR and BET measurements done on dried samples. TOC analyses of supernatant after adsorption experiments of HA onto 1 – 75 g/L NP.	IEP of α-Al_2O_3, γ-Al_2O_3 and TiO_2 were 5.5, 7.1 and 5.9, repsectively. ZnO, P-SiO_2 and S-SiO_2 were negative at all pH tested. HA reduced the EPM of all NP tested at all pH ranges but not always became negatively charged. Adsorption of HA, normalized by BET surface area, were 0.46, 0.28, 0.67 and 0.85 mg TOC/m^2 for TiO_2, γ-Al_2O_3, ZnO and α-Al_2O_3, respectively (same order of magnitude as inorganic minerals). Nano SiO_2 did not adsorb significant amounts of HA.
Zhang, et al. [22]	TiO_2, NiO, ZnO, Fe_2O_3, SiO_2 NP nominal diameter 15, 10-20, 50-70, 5-25, 10 nm, DLS diameter in water 530, 750, 320, 200, 740 nm in 1g/L stock solution, respectively.	SRNOM 0-10 mg/L	KCl 10 mM, pH 7.8 (adjusted with 0.1 M NaOH) $CaCl_2$ 0-8 mM	Adsorption experiments 10 mg/L SRNOM and 10-50 mg/L MeO. Microwave assisted digestion and GFAA for metal content. DLS and EPM in 10 mg/L MeO After addition of 0-10 mg/L SRNOM Adsorption experiments, DLS and EPM in 10 mg/L	The size of all particles increased with addition of 10 mM KCl at pH 7.8 excep SiO_2. 10 mg/L SRNOM hindered aggregation and EPM were all negative. TiO_2 and ZnO were more efficiently stabilized. In presence of 4 mg/L SRNOM, Ca^{2+} destabilized the particles (lowered EPM and increased aggregation rate) in the order Fe_2O_3, TiO_2, ZnO and NiO. SIO_2 remained stable.

Reference	Particles type, initial size and concentration	NOM	Electrolytes, pH and temp	Type of measurement for stability and interaction with NOM - instrument	Results and analysis
				MeO after addition of 4 mg/L SRNOM and 0-8 mM $CaCl_2$	
Zhang, et al. [23]	Nominal sizes in nm TiO_2 15 and 40, Fe_2O_3 5-25, ZnO 50-70, NiO 10-20, SiO_2 10, Fe_2O_3 80-90. DLS diameters 1g/L 530, 200, 200, 320, 750, 740, 85 nm respectively.	Tap water TOC 0-8.9 mg/L	Tap water, pH 8.1, conductivity 750-940 uS/cm, hardness 69-290 mg/L as $CaCO_3$, Alkalinity 56-210 mg/L as $CaCO_3$, Fluoride 0.10-0.82 mg/L. Buffer 0.01 NaHCO3, pH 8.2. 0.1M MgCl2. Alum ($Al_2(SO_4)_3.16H_2O$) 20-60 mg/L	Jar tests of rapid mixing followed by slow mixing of 10 mg/L NP. For TiO_2 and Fe_2O_3 an extra step of 0.45 um filtration. IEP in a range of pH in ultrapure water. EPM in tap water and ultrapure water (10 mM KNO_3). Mass residual in the water column after coagulation, flocculation and sedimentation measured by digestion followed by GFAA. Residual size was measured using DLS (0.002-3 um) and MFI (3-400 um).	IEP 5.2, 5.2, 6.5, 9.2, 9.1, 1.8, 8.4 respectively. All particles presented negative EPM in tap water even if below IEP probably due to organic matter coating. Addition of $MgCl_2$ and Alum removed max 80% of the mass of NP. Filtering of TIO_2 removed 92-99% mass of the initial particles. Fe_2O_3 remained mostly in the primary size and removal with filtration (no alum) reached only 20%.

DLS: Dynamic light scattering; tr-DLS: time resolved – Dymanic light scattering; FCS: Fluorescence correlation spectroscopy; EPM: Electrophoretic mobility; TEM: transmission electron microscopy; ICP-OES: Inductive coupled plasma- Optical emission spectrometry; GFAA: Graphite-furnace atomic absorption; SLS: Static light scattering; XPS: X-ray photoelectron spectroscopy; MFI: micro-flow imaging

CCC: critical coagulation concentration; MW: molecular weight; IS: ionic strength; IEP: isoelectric point; WWTP: wastewater treatment plant; TOC: Total organic carbon; SRHA: Suwannee river humic acid; SRFA: Suwannee river fulvic acid; SRNOM: Suwannee river natural organic matter; PDMS: Polydimethylsiloxane; MES: 2-(n-morpholino) ethenesulfonic acid; HEPES: 4-(2-hydroxyethtl)-1-piparazeneethanesulfonic acid; NT: Nanotubes; Df: fractal dimension.

Figure S1. Variations in stability ratio, W, at different values of pH (rows), concentration of NOM (rows), type of electrolyte (symbols) and salt additions (x-axes). The concentration TiO2 NP were kept at 100 mg/L.

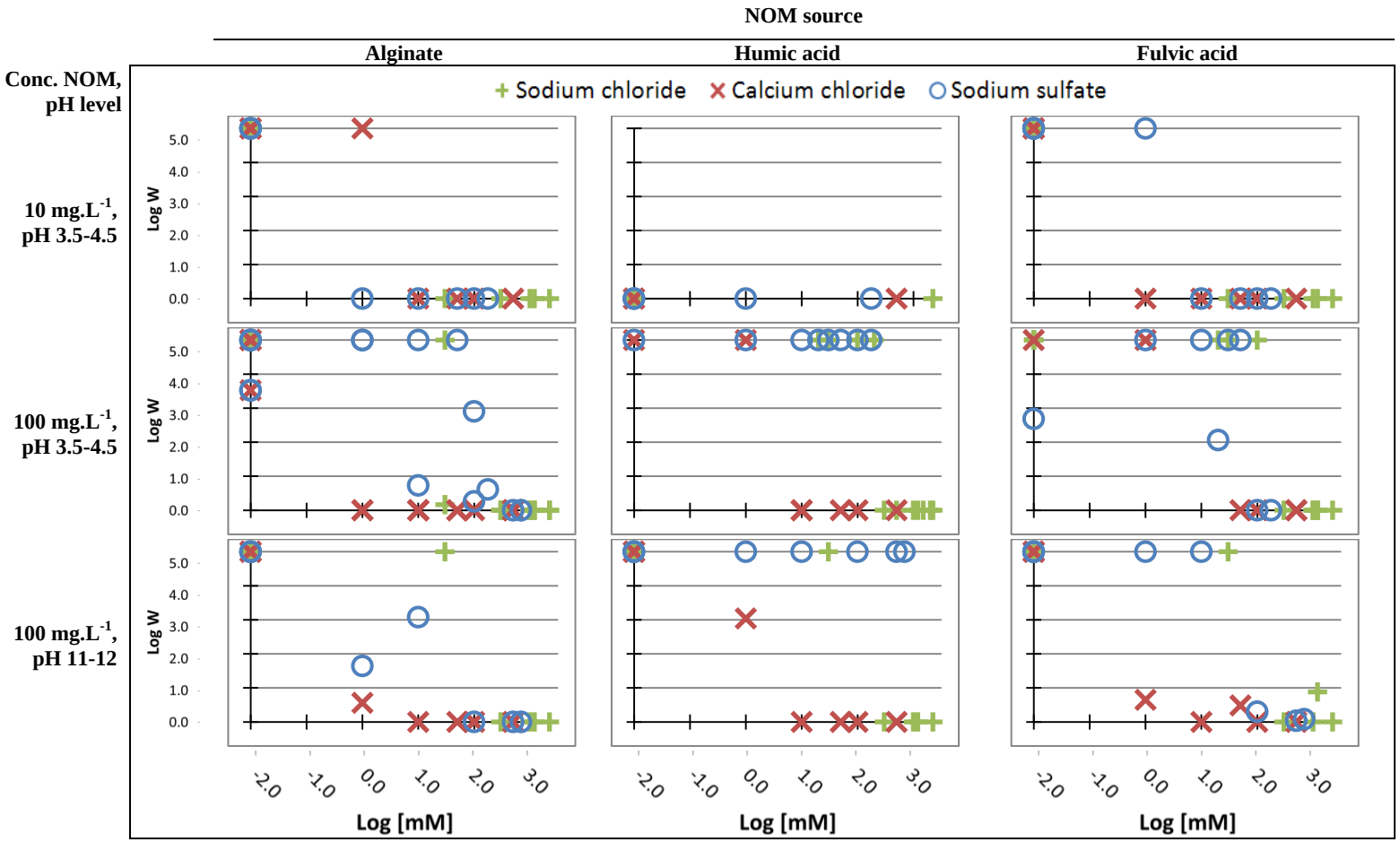

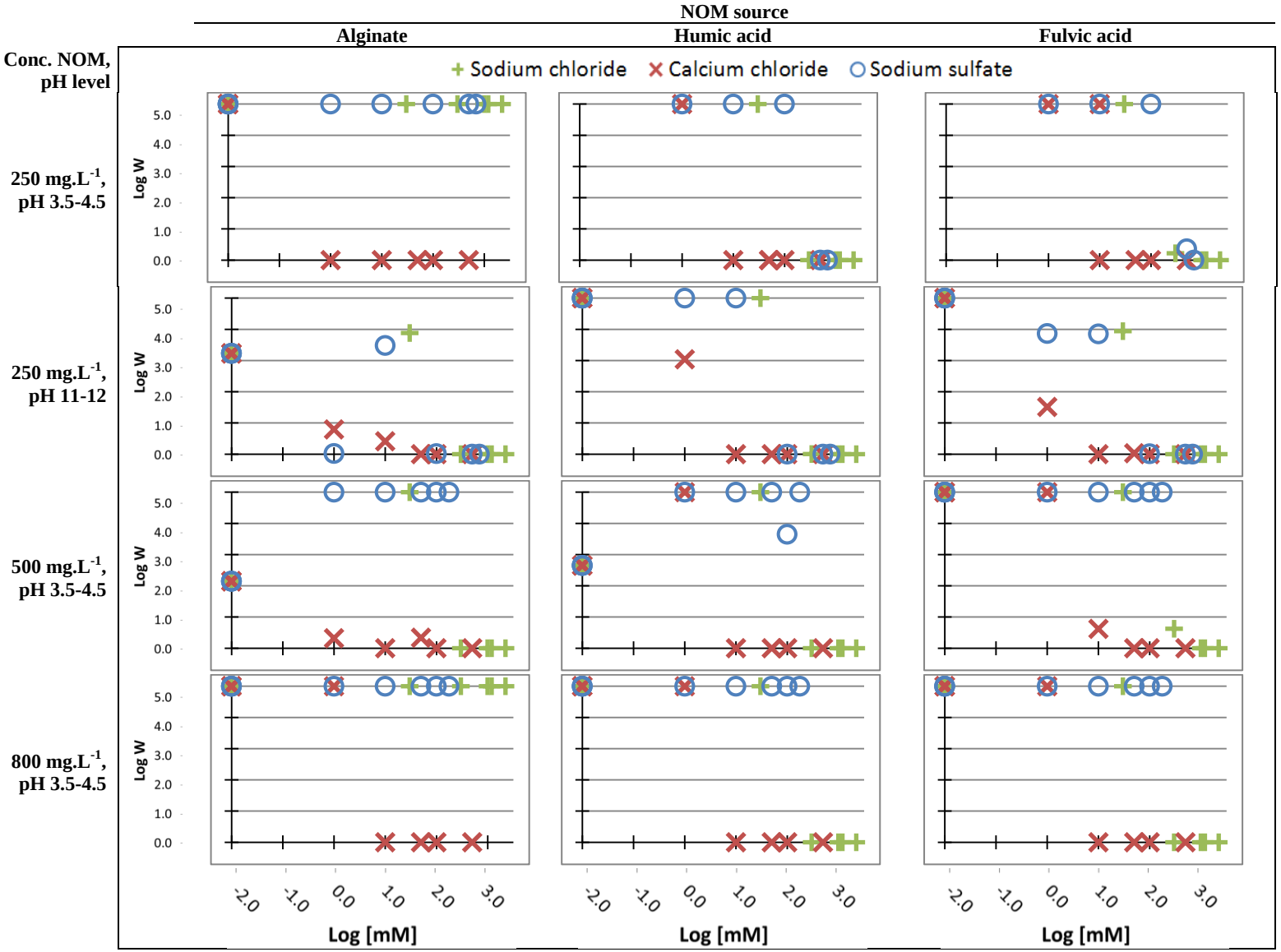
NOM source
Alginate
Humic acid
Fulvic acid
Conc. NOM, pH level
Sodium chloride
Calcium chloride
Sodium sulfate
250 mg.L-1, pH 3.5-4.5
250 mg.L-1, pH 11-12
500 mg.L-1, pH 3.5-4.5
800 mg.L-1, pH 3.5-4.5
Log W
5.0
4.0
3.0
2.0
1.0
0.0
-2.0
-1.0
0.0
1.0
2.0
3.0
Log [mM]

S.1. Equations used for repulsion and attraction in DLVO calculations

In all the cases considered here the common parameter is the Debye length, 1/κ, where κ is called the Debye-Hückel parameter and is defined as:

$$\frac{1}{\kappa} = \sqrt{\frac{\varepsilon\varepsilon_0 k_B T}{\sum_i (n_i)_0 \, z_i^2 e_0^2}}$$

Where $(n_i)_0$ is the concentration if the ith ion in the bulk phase and z_i is its valence, e_0 is the elementary charge (1.602E-19 C), ε is the dielectrically constant for the medium, ε_0 is the permittivity for vacuum (8.85E-12 C^2/J.m), kB is Boltzmanns constant (1.38E-23 $m^2.kg.s^{-2}.K^{-1}$) and T is the temperature in K.

Dielectric constant of water is very little affected by salt concentration. For water at 25°C it is 80 and for a saturated salt solution at 25°C is 81.5.

<u>Repulsive potential:</u>

Derjaguin approximation from equation 12.14 for moderate potentials between unequal spheres in Ohshima [24]:

$$V(R) = \frac{4.\pi.a_1.a_2.\varepsilon.\varepsilon_0.\left({k_B.T}/{z.e_0}\right)^2}{(a_1+a_2)}$$
$$\times\Bigg[Y_+^2\cdot\ln(1+e^{-\kappa.H}) + Y_-^2\cdot\ln(1-e^{-\kappa.H}) - \frac{1}{48}\cdot(Y_+^4+3\cdot Y_+^2\cdot Y_-^2)\cdot\left(\frac{\kappa.H}{2}\right)$$
$$\cdot\left\{1-tanh\left(\frac{\kappa.H}{2}\right)\right\} + \frac{1}{48}\cdot(Y_-^4+3\cdot Y_+^2\cdot Y_-^2)\cdot\left(\frac{\kappa.H}{2}\right)\cdot\left\{coth\left(\frac{\kappa.H}{2}\right)-1\right\}$$
$$-\frac{Y_+^4\cdot\left(1-\left(\frac{\kappa.H}{2}\right)\cdot tanh\left(\frac{\kappa.H}{2}\right)\right)}{96\cdot cosh^2\left(\frac{\kappa.H}{2}\right)} - \frac{Y_-^4\cdot\left(\left(\frac{\kappa.H}{2}\right)\cdot coth\left(\frac{\kappa.H}{2}\right)-1\right)}{96\cdot sinh^2\left(\frac{\kappa.H}{2}\right)} - \frac{Y_+^2}{5760}$$
$$\cdot\left\{Y_-^4+\frac{15}{8}\cdot Y_+^2\cdot(7\cdot Y_-^2+Y_+^2)\right\}\cdot\left(\frac{\kappa.H}{2}\right)\cdot\left\{coth\left(\frac{\kappa.H}{2}\right)-1\right\} + Y_+^6$$
$$\cdot\frac{17+4\cdot\left(\frac{\kappa.H}{2}\right)\cdot tanh\left(\frac{\kappa.H}{2}\right)}{46080\cdot cosh^2\left(\frac{\kappa.H}{2}\right)} - Y_-^6\cdot\frac{17+4\cdot\left(\frac{\kappa.H}{2}\right)\cdot coth\left(\frac{\kappa.H}{2}\right)}{46080\cdot sinh^2\left(\frac{\kappa.H}{2}\right)} + Y_+^4\cdot Y_-^2$$
$$\cdot\frac{1+\left(\frac{\kappa.H}{2}\right)\cdot tanh\left(\frac{\kappa.H}{2}\right)}{1024\cdot cosh^2\left(\frac{\kappa.H}{2}\right)} - Y_+^2\cdot Y_-^4\cdot\frac{1+\left(\frac{\kappa.H}{2}\right)\cdot coth\left(\frac{\kappa.H}{2}\right)}{1024\cdot sinh^2\left(\frac{\kappa.H}{2}\right)} - Y_+^6$$
$$\cdot\frac{1-11\cdot\left(\frac{\kappa.H}{2}\right)\cdot tanh\left(\frac{\kappa.H}{2}\right)}{15360\cdot cosh^2\left(\frac{\kappa.H}{2}\right)} + Y_-^6\cdot\frac{1+11\cdot\left(\frac{\kappa.H}{2}\right)\cdot coth\left(\frac{\kappa.H}{2}\right)}{15360\cdot sinh^2\left(\frac{\kappa.H}{2}\right)}\Bigg]$$

With

$$Y_+ = \frac{y_{01}+y_{02}}{2} \quad , \quad Y_- = \frac{y_{01}-y_{02}}{2}$$

Where V(R) is the potential as a function of the interparticle separation, H is the surface to surface distance and y_0 is the scaled surface electrical potential ($z.e.\psi_0/k_B.T$), z is the valence of ions, a_i is the radii of the spheres.

<u>Attractive potential:</u>

The repulsion is calculated using the equation [25]:

$$V(R) = -\frac{A}{6}\cdot\left(\frac{2\cdot a_1\cdot a_2}{h^2+2\cdot a_1\cdot h+2\cdot a_2\cdot h} + \frac{2\cdot a_1\cdot a_2}{h^2+2\cdot a_1\cdot h+2\cdot a_2\cdot h+4\cdot a_1\cdot a_2} + ln\left(\frac{h^2+2\cdot a_1\cdot h+2\cdot a_2\cdot h}{h^2+2\cdot a_1\cdot h+2\cdot a_2\cdot h+4\cdot a_1\cdot a_2}\right)\right)$$

Where A is the Hamaker coefficient in J.

S.2. Chracteristics of the natural organic matter

The following information is a compilation obtained from the sources of NOM used:

PRONOVA UP LVG (ultrapure, low viscosity, high-G sodium alginate) from Novamatrix[26] is a linear polysaccharide which consists of (1→4)-linked β-D-mannuronate (M) and its C-5 epimer α-L-guluronate (G). The properties provided by the manufacturer are summarized below.

Property	Value
Apparent viscosity	163 mPa.s
pH	7
Guluronic acid content	68% (weight)
Heavy metal content	< 6 ppm (weight)

Humic and fulvic acid standards were obtained from the International Humic Substances Society (IHSS, University of Minnesota, St. Paul, MN, USA) batches 2S101H and 2S101F, respectively. The properties provided by the supplier are summarized in the following lines [27]. The overall charge per unit of mass is presented in figure S2.

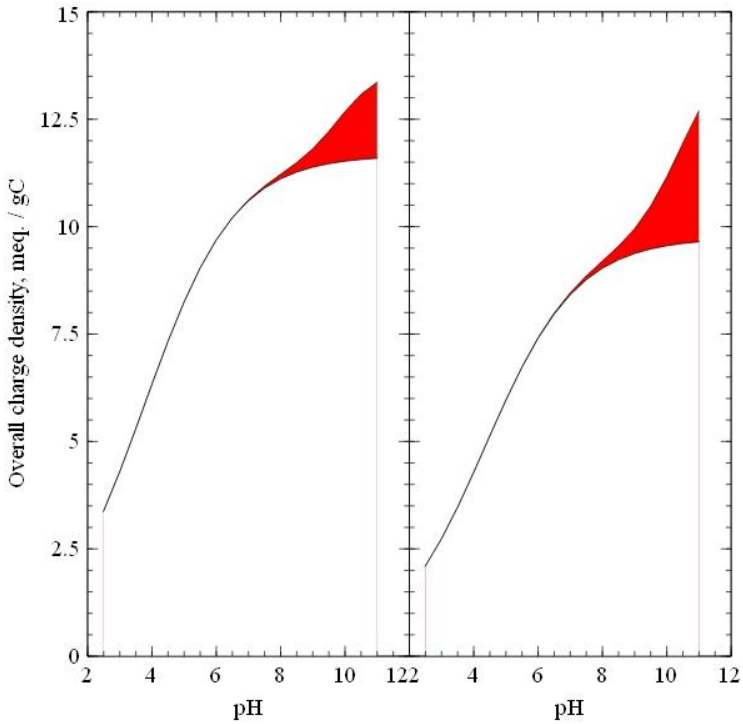

Figure S2. Overall charge density variation as a function of pH for Fulvic acid (left) and Humic acid (right). The shadowed region indicates the influence of the phenolic groups. The values were obtained using the modified Henderson-Hasselbalch equation and the parameters provided by the IHSS[27].

Elemental composition:

Sample	H_2O	Ash	C	H	O	N	S	P
HA	20.4	1.04	52.63	4.28	42.04	1.17	0.54	0.013
FA	16.9	0.58	52.34	4.36	42.98	0.67	0.46	0.004

S.3. Characterization of TiO_2 NP obtained from hydrolytic synthesis

Dialysis and aging temperature (°C)	Crystalline structure and composition		Particle size (diameter, nm)			
	% Anatase	% Brookite	Scherrer crystallite size, X-ray diffraction	Transmission electron microscopy	Dynamic light scattering	Electrospray – Scanning Mobility Particle Sizer
0	94.8 ± 1.3	5.2 ± 1.3	3.9 ± 0.1	≈ 4	7.8 ± 0.6	8.6 ± 0.8
5	91.8 ± 0.4	8.3 ± 0.4	4.0		10.2 ± 0.4	9.2 ± 1.6
20-23	92.3	7.5	4.2 ± 0.1		18.0	18.5 ± 2.4

Note: In all three cases, reaction temperature is 0°C.

The NP used in the aggregation experiments and pH corresponds to the aging temperature of 20°C.

S.4. References

1. G. Chen, X. Liu and C. Su, *Environmental Science & Technology*, 2012, 120604054616000.
2. I. Chowdhury, S. L. Walker and S. E. Mylon, *Environmental Science: Processes & Impacts*, 2013, **15**, 275-282.
3. R. F. Domingos, C. Peyrot and K. J. Wilkinson, *Environmental Chemistry*, 2010, **7**, 61.
4. R. F. Domingos, N. Tufenkji and K. J. Wilkinson, *Environmental Science & Technology*, 2009, **43**, 1282-1286.
5. R. A. French, A. R. Jacobson, B. Kim, S. L. Isley, R. L. Penn and P. C. Baveye, *Environmental Science & Technology*, 2009, **43**, 1354-1359.
6. A. A. Keller, H. Wang, D. Zhou, H. S. Lenihan, G. Cherr, B. J. Cardinale, R. Miller and Z. Ji, *Environmental Science & Technology*, 2010, **44**, 1962-1967.
7. J. Labille, J. Feng, C. Botta, D. Borschneck, M. Sammut, M. Cabie, M. Auffan, J. Rose and J.-Y. Bottero, *Environmental Pollution*, 2010, **158**, 3482-3489.
8. S. Li and W. Sun, *Journal of Hazardous Materials*, 2011, **197**, 70-79.
9. X. Liu, G. Chen and C. Su, *Journal of Colloid and Interface Science*, 2011, **363**, 84-91.
10. W. Liu, W. Sun, A. G. L. Borthwick and J. Ni, *Colloids and Surfaces A: Physicochemical and Engineering Aspects*, 2013.
11. H. H. Liu, S. Surawanvijit, R. Rallo, G. Orkoulas and Y. Cohen, *Environmental Science & Technology*, 2011, **45**, 9284-9292.
12. F. Loosli, P. Le Coustumer and S. Stoll, *Water Research*, 2013, **47**, 6052-6063.
13. I. a. Mudunkotuwa and V. H. Grassian, *Journal of the American Chemical Society*, 2010, **132**, 14986-14994.
14. S. Ottofuelling, F. Von Der Kammer and T. Hofmann, *Environmental Science & Technology*, 2011, **45**, 10045-10052.
15. Y.-h. Shih, C.-m. Zhuang, Y.-H. Peng, C.-h. Lin and Y.-m. Tseng, *Science of the Total Environment*, 2012, **435–436**, 446-452.
16. Y.-H. Shih, W.-S. Liu and Y.-F. Su, *Environmental Toxicology and Chemistry*, 2012, **31**, 1693-1698.
17. M. Sillanpää, T.-M. Paunu and P. Sainio, *Journal of Physics: Conference Series*, 2011, **304**, 012018.
18. N. Solovitch, J. Labille, J. Rose, P. Chaurand, D. Borschneck, M. R. Wiesner and J. Y. Bottero, *Environ Science & Technology*, 2010, **44**, 4897-4902.
19. B. J. R. Thio, D. Zhou and A. A. Keller, *Journal of Hazardous Materials*, 2011, **189**, 556-563.
20. F. von der Kammer, S. Ottofuelling and T. Hofmann, *Environmental Pollution*, 2010, **158**, 3472-3481.
21. K. Yang, D. Lin and B. Xing, *Langmuir*, 2009, **25**, 3571-3576.

22. Y. Zhang, Y. Chen, P. Westerhoff and J. Crittenden, *Water Research*, 2009, **43**, 4249-4257.
23. Y. Zhang, Y. Chen, P. Westerhoff, K. Hristovski and J. C. Crittenden, *Water Research*, 2008, **42**, 2204-2212.
24. H. Ohshima, *Biophysical chemistry of biointerfaces*, Wiley, Hoboken, NJ, USA, 2010.
25. W. B. Russel, D. A. Saville and S. W., *Colloidal dispersions*, Cambridge, 1989.
26. NovaMatrix - FMC corporation, *Product information bulletin - Alginate stability*, FMC corporation, 2002.
27. International Humic Substances Society, *International Humic Substances Society*, http://www.humicsubstances.org/, 2013.